First High-Convergence Cryogenic Implosion in a Near-Vacuum Hohlraum

L. F. Berzak Hopkins,[1] N. B. Meezan,[1] S. Le Pape,[1] L. Divol,[1] A. J. Mackinnon,[1] D. D. Ho,[1] M. Hohenberger,[2] O. S. Jones,[1] G. Kyrala,[3] J. L. Milovich,[1] A. Pak,[1] J. E. Ralph,[1] J. S. Ross,[1] L. R. Benedetti,[1] J. Biener,[1] R. Bionta,[1] E. Bond,[1] D. Bradley,[1] J. Caggiano,[1] D. Callahan,[1] C. Cerjan,[1] J. Church,[1] D. Clark,[1] T. Döppner,[1] R. Dylla-Spears,[1] M. Eckart,[1] D. Edgell,[2] J. Field,[1] D. N. Fittinghoff,[1] M. Gatu Johnson,[4] G. Grim,[3] N. Guler,[3] S. Haan,[1] A. Hamza,[1] E. P. Hartouni,[1] R. Hatarik,[1] H. W. Herrmann,[3] D. Hinkel,[1] D. Hoover,[5] H. Huang,[5] N. Izumi,[1] S. Khan,[1] B. Kozioziemski,[1] J. Kroll,[1] T. Ma,[1] A. MacPhee,[1] J. McNaney,[1] F. Merrill,[3] J. Moody,[1] A. Nikroo,[5] P. Patel,[1] H. F. Robey,[1] J. R. Rygg,[1] J. Sater,[1] D. Sayre,[1] M. Schneider,[1] S. Sepke,[1] M. Stadermann,[1] W. Stoeffl,[1] C. Thomas,[1] R. P. J. Town,[1] P. L. Volegov,[3] C. Wild,[6] C. Wilde,[3] E. Woerner,[6] C. Yeamans,[1] B. Yoxall,[1] J. Kilkenny,[5] O. L. Landen,[1] W. Hsing,[1] and M. J. Edwards[1]

[1]*Lawrence Livermore National Laboratory, Livermore, California 94550, USA*
[2]*Laboratory for Laser Energetics, University of Rochester, Rochester, New York 14623, USA*
[3]*Los Alamos National Laboratory, Los Alamos, New Mexico 87545, USA*
[4]*Plasma Science and Fusion Center, Massachusetts Institute of Technology, Cambridge, Massachusetts 02139, USA*
[5]*General Atomics, San Diego, California 93286, USA*
[6]*Diamond Materials GMBH, Freiburg, Germany*

(Received 16 January 2015; published 29 April 2015)

Recent experiments on the National Ignition Facility [M. J. Edwards *et al.*, Phys. Plasmas 20, 070501 (2013)] demonstrate that utilizing a near-vacuum hohlraum (low pressure gas-filled) is a viable option for high convergence cryogenic deuterium-tritium (DT) layered capsule implosions. This is made possible by using a dense ablator (high-density carbon), which shortens the drive duration needed to achieve high convergence: a measured 40% higher hohlraum efficiency than typical gas-filled hohlraums, which requires less laser energy going into the hohlraum, and an observed better symmetry control than anticipated by standard hydrodynamics simulations. The first series of near-vacuum hohlraum experiments culminated in a 6.8 ns, 1.2 MJ laser pulse driving a 2-shock, high adiabat ($\alpha \sim 3.5$) cryogenic DT layered high density carbon capsule. This resulted in one of the best performances so far on the NIF relative to laser energy, with a measured primary neutron yield of 1.8×10^{15} neutrons, with 20% calculated alpha heating at convergence $\sim 27\times$.

DOI: 10.1103/PhysRevLett.114.175001 PACS numbers: 52.57.Fg, 52.38.Ph, 52.70.La, 52.70.Nc

Inertial confinement fusion (ICF) experiments implode millimeter-scale deuterium-tritium (DT) filled spherical capsules, compressing and heating the DT fuel to fusion conditions and releasing energy [1]. Indirect-drive ICF places the fuel-filled capsule at the center of a high-Z radiation enclosure (hohlraum) and strikes the inside walls of the hohlraum with laser power. This produces an internal bath of x rays—a radiation drive which ablates and implodes the fuel-filled capsule. The National Ignition Facility (NIF) [2,3] drives this process using 192 frequency-tripled laser beams (351 nm at 3ω), which enter a cylindrical hohlraum through laser entrance holes (LEHs) at each end. The laser beams are pointed through the LEHs to provide various angles of drive to the capsule such that the superposition of drives can be spherically symmetric throughout the implosion time.

Typically, ICF experiments on the NIF have utilized plastic (CH) capsules inside gold hohlraums filled with helium at densities ranging from 0.96 [4] to 1.6 mg/cm^3 [5]. To reach ignition conditions with this capsule, laser pulses on the order of 15–20 ns in length are required [6]. Although vacuum hohlraums were initially considered, the long pulse duration for CH capsules led to choosing higher densities of hohlraum fill [7,8] to minimize expansion of the interior gold wall [Fig. 1(a)] [9]. The intended effect is to maintain an open path for laser propagation to the wall for the full pulse duration.

In this Letter, we report on the first experimental campaign on the NIF using near-vacuum hohlraums (NVH) to drive a high convergence cryogenic DT layered capsule implosion. A NVH has a hohlraum fill density of 0.03 mg/cm^3 helium, more than an order of magnitude lower density than conventional gas-filled hohlraums (0.96–1.6 mg/cm^3). Symmetry of implosions driven with the NVH is controlled through direct adjustments to the inner and outer beam power balance rather than relying on beam wavelength separations [10] and the resultant cross-beam energy transfer [11,12]. Unlike earlier research on true "vacuum" hohlraums [13–15], the NVH maintains a nonzero gas fill, confined by thin windows at the LEH, which both allows for cryogenic layering operation and protects the hohlraum axis from a stagnation feature caused

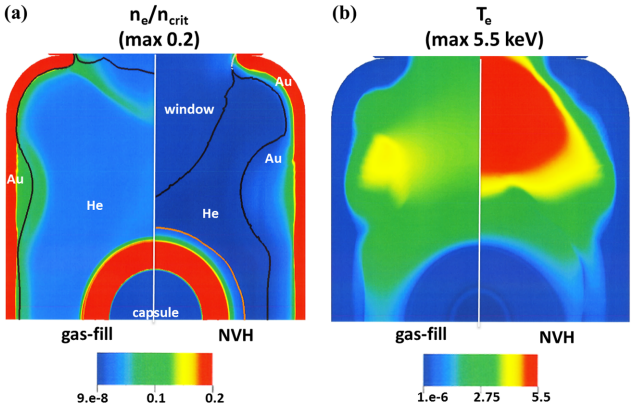

FIG. 1 (color online). Simulated equatorial view of upper halves of gas-filled (0.96 mg/cm^3) and NVH hohlraums near peak power in a 5 ns laser pulse, comparing (a) material boundaries and electron density to critical density ratio—the higher density gas fill (left halves) minimizes wall and window motion, while the low density NVH allows the wall and window to expand (right halves). (b) Electron temperature; pressure equilibrium leads to a lower density and higher temperature inside the NVH.

by wall expansion during the laser pulse. Usage of the NVH for capsule implosions was first experimentally investigated in single-shock, indirect drive plastic (CH) exploding pusher experiments (IDEP) [16], demonstrating a high efficiency platform for a 5× convergence round implosion driven by a relatively short 4.5 ns pulse (325 TW peak power, 0.93 MJ).

Here we report on our early success at pushing the NVH to drive a 2-shock, high adiabat ($\alpha \sim 3.5$ in units of the Fermi degenerate pressure) cryogenic DT layered high-density carbon (HDC) implosion to convergence ~27×, while keeping the implosion symmetry under control. While such a design using a 6.8 ns laser pulse cannot reach ignition (the adiabat is too high to reach the requisite level of fuel compression at the designed implosion velocity), current hydrodynamics calculations support 2 or 3-shock HDC implosion designs that could reach significant alpha-heating (or even ignition) with laser pulses as short as 8–9 ns (i.e., only 20% longer) in a NVH.

The ability of any hohlraum to drive the fuel-filled capsule to fusion-relevant conditions can be modeled by a source-sink relation: $P_L \propto \sigma T_r^4 A_{\rm cap}$, where P_L is the laser input power, σT_r^4 is the spectrally integrated radiation flux inside the hohlraum, and $A_{\rm cap}$ is the area of the capsule. In practice, not all of the input laser power is available to drive the capsule, so the source-sink equation becomes [13,17]

$$\eta_{\rm CE}(\gamma P_L - P_{\rm BS}) = \sigma T_r^4[(1-\alpha)A_{\rm wall} + A_{\rm LEHs} + A_{\rm cap}]. \quad (1)$$

In Eq. (1), $\eta_{\rm CE}$ is the laser to x-ray conversion efficiency and encompasses energy stored in the hohlraum gas and corona. $P_{\rm BS}$ accounts for laser power scattered out of the hohlraum via stimulated Brillouin or stimulated Raman backscatter [18] and no longer available for conversion to x-ray drive. $A_{\rm wall}$ is the area of the hohlraum wall, and α is the wall reflectivity (albedo) [19]. $A_{\rm LEHs}$ is the area of the LEHs. The $\eta_{\rm CE}$ term is calculated self-consistently in radiation hydrodynamics simulations and was inferred to be 90% at peak power in empty hohlraum experiments on the NIF [14,20]. Measured x-ray flux at peak drive in the NVH is consistent with Eq. (1), $\eta_{\rm CE} \sim 90\%$, $\alpha \sim 90\%$ in line with [14]. We use γ as an empirical degradation factor, $\gamma < 1$ [21,22], required to match experimentally measured capsule implosion performance to simulations with the radiation-hydrodynamics code HYDRA [23]. For gas-filled hohlraums, $P_{\rm BS}$ is typically on the order of $15\%P_L$, reducing laser-hohlraum coupling to 85% [Fig. 2(a)] [24]. Figure 1 shows a key feature of NVH evolution: the hohlraum does not stay near empty for long, but reaches a pressure equilibrium at roughly half the electron density [Fig. 1(a)] with an electron temperature 50% higher (5–6 keV versus 3–4 keV) than a gas-filled hohlraum [Fig. 1(b)]. Consequently, stimulated Brillouin and stimulated Raman linear gain estimates, which scale as (n_e/T_e) [25], are reduced. The measured $P_{\rm BS}$ is reduced to 1%–$3\%P_L$ for pulse lengths varying from 4.5–7 ns with laser energies from 0.93–1.6 MJ [Fig. 2(a)], allowing the NVH to achieve 97%–99% laser-hohlraum coupling.

Furthermore, in gas-filled hohlraums, an empirical and time-varying γ coefficient is required to match experimental measurements with 2D integrated hohlraum-capsule HYDRA simulations using a detailed configuration accounting high flux model [21,27]. The γ coefficient is typically of order 0.72–0.78, degrading the flux available to drive the capsule by nearly 30%. The origin of this

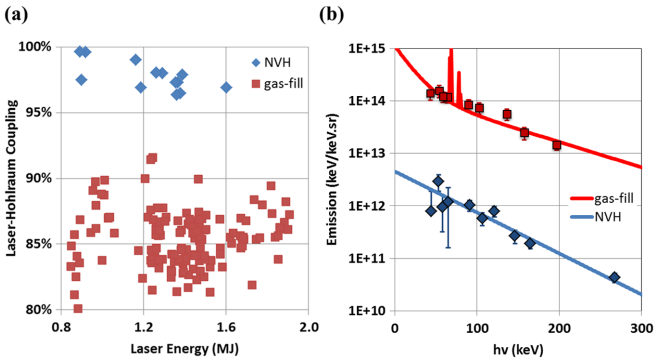

FIG. 2 (color online). (a) Comparison of experimental laser-hohlraum coupling for NVH (average of 97.8% with a standard deviation of 0.011) relative to gas-filled cryogenic cylindrical hohlraum experiments (average of 85.4% with a standard deviation of 0.022) measured through NIF's suite of backscatter diagnostics [24,26]. (b) Comparison of measured, time-integrated hard x-ray FFLEX data (see text) for a NVH (N131212, blue) and a gas-filled hohlraum (N130628, red) HDC experiment with similar laser energies; the NVH shows approximately a 100× reduction in suprathermal electron generation.

disagreement between simulations and experiments is not presently well understood and is an area of active research; the work reported here suggests that it is related to the hohlraum gas fill. Potential sources of this disagreement include lower than expected (by current models) electron heat conduction or energy stored in the hohlraum through heating the gas, in Langmuir waves, or in suprathermal electrons. In all our NVH experiments, a γ coefficient of order 0.9 is suitable for matching measured implosion parameters. The small remaining deviation from unity is likely compensating for uncertainty in the modeling of atomic physics and equations of state.

As a result, the NVH provides 30%–40% more x-ray drive to accelerate the capsule relative to high gas density filled hohlraums with similar laser energies. This efficiency increase can be seen in Fig. 3, which compares laser pulses of similar peak power and energy (250 TW, 700 kJ, HDC capsule) used for gas-filled hohlraum (red) and NVH (blue) experiments with the resulting hohlraum internal radiation temperature tuned to experimental measurements (here, shock velocities, and accelerations). Laser drive in the NVH results in a peak radiation temperature more than 20 eV higher than the gas-filled hohlraum. This simulated temperature difference is confirmed by the different peak x-ray fluxes for these two experiments measured through the hohlraum LEH by Dante [28] and corrected for the LEH closure measured by the soft x-ray imager [29,30]. The rise to peak radiation temperature is also faster in the NVH relative to the gas-filled hohlraum, resulting in 2.5× more flux during the rise to peak power and 1.5× more flux at peak.

An additional benefit of the NVH is the observed minimal generation of suprathermal (>170 keV) electron preheat. These energetic electrons are believed to be generated through two-plasmon decay [31] and stimulated Raman scattering in gas-filled hohlraums and may degrade implosion performance of a cryogenic fuel layer by decompressing the fuel [32]. The Filter-Fluorescer Experiment (FFLEX) diagnostic measures hard x-ray bremsstrahlung emission over specific energy bands and is used to infer suprathermal electron generation [33]. A conventional gas-filled hohlraum with a 1.2 MJ (4-shock) drive generated nearly 1 kJ of suprathermal electrons; in comparison, 1.2 MJ (2-shock) drive in the NVH generated approximately 10 J. Suprathermal electrons also introduce a high background on diagnostics, limiting measurement capabilities; the low x-ray background of the NVH improves signal measurements, presenting new implosion diagnostic opportunities, for example with Compton radiography or proton time-of-flight detectors [34] to measure fuel-ablator density variations.

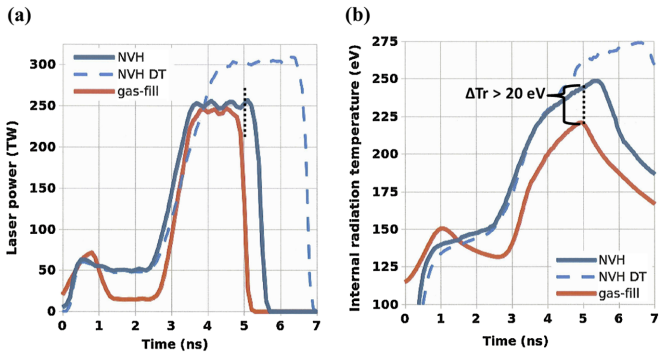

FIG. 3 (color online). Comparison of laser pulses (a) and the resulting simulated hohlraum internal radiation temperature (b) from a recent 3-shock, gas-filled HDC shock-timing experiment, N131202 (red), with a 2-shock, NVH HDC shock-timing experiment, N130916 (blue). The 3-shock plots have been shifted in time to align the rises to peak power. Despite using similar peak laser powers and energies, the NVH peak drive is >20 eV higher than the gas-filled drive, resulting in 50% more hohlraum flux in the NVH. The dashed blue traces denote the laser and temperature for the DT cryogenic layer experiment N131212.

Because HDC is more than 3 times as dense as CH (3.42 g/cm^3 vs 1.1 g/cm^3 relatively) [35], thinner capsules can be driven by shorter drives to ignition-relevant conditions [22], making HDC a natural ablator choice for cryogenic layered implosion in the NVH. For this proof-of-principle campaign, we chose a 2-shock drive (dotted, blue trace in Fig. 3) that has very low growth for ablation front Rayleigh-Taylor instabilities [36–38] and is robust to shock mistiming. The resulting cryogenic DT layered implosion—shot N131212—utilized an 85 μm undoped HDC capsule with a 6.8 ns laser pulse (305 TW peak power, 1.164 MJ) to achieve a neutron yield of 1.8×10^{15} [39] with no evidence of capsule material mixing into the hot spot [40]. This yield is consistent with an enhancement due to alpha heating of approximately 20%, inferred from the measurement-based hot spot model [41] as well as from HYDRA calculations. The increased efficiency of the NVH is evident by noting that the gas-filled hohlraum experiments with comparable neutron yields required laser energies greater than 1.5 MJ, nearly 30% higher than used for N131212. Shot N131212 achieved 27× convergence with an inferred hot spot pressure of 100 Gbar. Laser-hohlraum coupling remained high at 99% (11.7 kJ measured backscatter out of 1164 kJ of incident laser energy) with negligible suprathermal electron generation [Fig. 2(b)].

Beside delivering high hohlraum efficiency and little signature of laser-plasma interaction processes, a combination of neutron and x-ray images demonstrate an adequate level of symmetry control during the stagnation phase of the implosion. Earlier work [7] anticipated uncontrollable symmetry swings in vacuum hohlraums (due to fast and nonuniform expansion of the hohlraum wall) and early loss of inner beam propagation (due to hohlraum filling). However, the time-integrated x-ray emission measured a 24% prolate hot spot (as fit with the 2nd Legendre moment, $P2$), (Fig. 4), with a radius $P0 = 35.9$ μm, indicating that the drive to the capsule waist

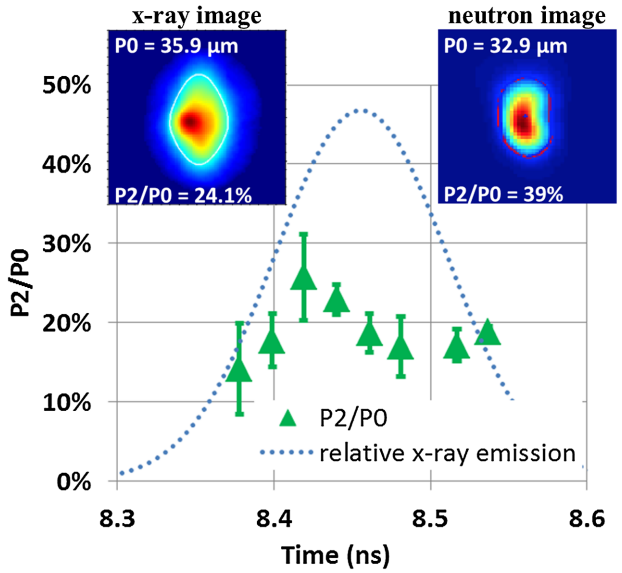

FIG. 4 (color online). Measured $P2/P0$ during x-ray emission, showing minimal symmetry swing of the hot spot during x-ray emission. The left image is a measured time-integrated equatorial x-ray emission, showing a prolate hot spot. The right image is a measured time-integrated neutron emission, showing a prolate core.

from the inner beams was not only adequate but needs to be reduced in subsequent implosions to achieve a round hot spot. This measurement is consistent with better propagation of the inner cone laser beams inside the hohlraum relative to 2D integrated hohlraum-capsule HYDRA simulations. This is confirmed by time-integrated soft x-ray images of the hohlraum wall through the LEH [30], which show brighter inner cone laser spots at the hohlraum waist relative to simulations as well. The primary DT neutron image (Fig. 4) is of similar size and shape ($P0 = 32.9$ μm, $P2/P0 = +39\%$) to the time-integrated x-ray image, suggesting that the hot spot shape is representative of the symmetry of the burning volume. More importantly, the time-resolved x-ray imaging of the implosion during burn (x-ray burn width $= 170 \pm 14$ ps, neutron burn width $= 161 \pm 30$ ps, as measured by GRH, gamma reaction history diagnostic [42]) shows minimal change (on the order of $\pm 5\%$) in symmetry. This result suggests that the assembled burning volume underwent minimal symmetry distortions near the time of stagnation.

Overall, implosion metrics, summarized in Table 1, are well matched by 2D integrated hohlraum-capsule HYDRA simulations using a detailed configuration accounting high flux model, adjusted for enhanced inner beam propagation.

To summarize, we have reported on the first high convergence cryogenic DT layered capsule implosion driven by a near-vacuum hohlraum. By using a high density ablator (HDC) material, the 2-shock 6.8-ns drive used, while nonigniting by design, has most of the characteristics of an igniting design that would require a finely tuned 8–9 ns pulse. Observables demonstrate the high efficiency and low level of laser plasma interaction effects, while showing implosion performance consistent with 2D HYDRA simulations. Implosion symmetry is controlled well, and inner cone beams propagate better than expected to the waist of the hohlraum, suggesting longer laser pulses (with corresponding lower adiabats and higher compression) are possible.

TABLE I. N131212 implosion metrics.

	2D Postshot simulation	Data
Neutron yield	1.8×10^{15}	1.8×10^{15}
Yield/simulated	99%	NA
Bang time (ns)	8.48	8.51 ± 0.03
DT Tion (keV)	3.1	3.5 ± 0.15[a]
Fuel vel. (km/s)	350	NA
Neutron burn width (ps)	149	161 ± 30
X-ray burn width (ps)	139	170 ± 14
Inferred stagnation pressure (Gbar)	103[b]	92 ± 7[c]

[a]Inferred from measured neutron spectrum width.
[b]Burn-averaged weighted by the burning volume.
[c]Inferred from integrated hot spot model [41].

Because of its high efficiency, low hot electron preheat, and better symmetry than expected, a broad range of experiments utilizing the NVH are currently being planned for physics studies on the NIF, as well as a tuning campaign using the NVH with HDC capsules, which seeks to achieve alpha-heating dominated neutron yields. A family of 2-shock ignition designs has been developed with adiabats ranging from 2.5–3.5, and pulse durations from 6.5–8 ns with simulated 1D yields from 100 kJ–4 MJ. The NVH opens the potential to explore this range of designs with a highly efficient system in a regime of hohlraum performance not previously predicted by simulations.

The authors would like to thank the NIF operations, laser, target fabrication, and diagnostic teams for their efforts during these experiments. This work was performed under the auspices of the U.S. Department of Energy by Lawrence Livermore National Laboratory under Contract No. DE-AC52-07NA27344.

[1] J. D. Lindl, P. Amendt, R. L. Berger, S. G. Glendinning, S. H. Glenzer, S. W. Haan, R. L. Kauffman, O. L. Landen, and L. J. Suter, Phys. Plasmas **11**, 339 (2004).
[2] E. I. Moses, R. N. Boyd, B. A. Remington, C. J. Keane, and R. Al-Ayat, Phys. Plasmas **16**, 041006 (2009).
[3] G. H. Miller, E. I. Moses, and C. R. Wuest, Nucl. Fusion **44**, S228 (2004).
[4] M. J. Edwards *et al.*, Phys. Plasmas **20**, 070501 (2013).
[5] O. A. Hurricane *et al.*, Nature (London) **506**, 343 (2014).
[6] S. Haan *et al.*, Phys. Plasmas **18**, 051001 (2011).

[7] S. W. Haan, S. M. Pollaine, J. D. Lindl, L. J. Suter, R. L. Berger, L. V. Powers, W. E. Alley, P. A. Amendt, J. A. Futterman, W. K. Levedahl *et al.*, Phys. Plasmas **2**, 2480 (1995).

[8] S. Laffite and P. Loiseau, Phys. Plasmas **17**, 102704 (2010).

[9] N. D. Delamater, T. J. Murphy, A. A. Hauer, R. L. Kauffman, A. L. Richard, E. L. Lindman, G. R. Magelssen, B. H. Wilde, D. B. Harris, B. A. Failor *et al.*, Phys. Plasmas **3**, 2022 (1996).

[10] S. H. Glenzer, B. J. MacGowan, P. Michel, N. B. Meezan, L. J. Suter, S. N. Dixit, J. L. Kline, G. A. Kyrala, D. K. Bradley, D. A. Callahan *et al.*, Science **327**, 1228 (2010).

[11] P. Michel, L. Divol, E. A. Williams, S. Weber, C. A. Thomas, D. A. Callahan, S. W. Haan, J. D. Salmonson, S. Dixit, D. E. Hinkel *et al.*, Phys. Rev. Lett. **102**, 025004 (2009).

[12] P. Michel, S. H. Glenzer, L. Divol, D. K. Bradley, D. Callahan, S. Dixit, S. Glenn, D. Hinkel, R. K. Kirkwood, J. L. Kline *et al.*, Phys. Plasmas **17**, 056305 (2010).

[13] L. J. Suter, R. L. Kauffman, C. B. Darrow, A. A. Hauer, H. Kornblum, O. L. Landen, T. J. Orzechowski, D. W. Phillion, J. L. Porter, L. V. Powers *et al.*, Phys. Plasmas **3**, 2057 (1996).

[14] R. E. Olson, L. J. Suter, J. L. Kline, D. A. Callahan, M. D. Rosen, S. N. Dixit, O. L. Landen, N. B. Meezan, J. D. Moody, C. A. Thomas *et al.*, Phys. Plasmas **19**, 053301 (2012).

[15] J. Shao-En, S. Ke-Xu, D. Yong-Kun, H. Tian-Xuan, C. Yan-Li, and C. Jiu-Sen, Chin. Phys. Lett. **22**, 2328 (2005).

[16] S. Le Pape, L. Divol, L. Berzak Hopkins, A. Mackinnon, N. B. Meezan, D. Casey, J. Frenje, H. Herrmann, J. McNaney, T. Ma *et al.*, Phys. Rev. Lett. **112**, 225002 (2014).

[17] J. Lindl, *Inertial Confinement Fusion* (Springer-Verlag, New York, 1998).

[18] O. L. Landen, R. Benedetti, D. Bleuel, T. R. Boehly, D. K. Bradley, J. A. Caggiano, D. A. Callahan, P. M. Celliers, C. J. Cerjan, D. Clark *et al.*, Plasma Phys. Controlled Fusion **54**, 124026 (2012).

[19] M. D. Rosen, in Proceedings of the Fundamentals of ICF hohlraums, *Lectures in the Scottish Universities Summer School in Physics, on High Energy Laser Matter Interactions*, 2005, edited by D. A. Jaroszynski, R. Bingham, and R. A. Cairns (CRC Press, Boca Raton, 2009), pp. 325–353.

[20] J. L. Kline, S. H. Glenzer, R. E. Olson, L. J. Suter, K. Widmann, D. A. Callahan, S. N. Dixit, C. A. Thomas, D. E. Hinkel, E. A. Williams *et al.*, Phys. Rev. Lett. **106**, 085003 (2011).

[21] O. S. Jones, C. J. Cerjan, M. M. Marinak, J. L. Milovich, H. F. Robey, P. T. Springer, L. R. Benedetti, D. L. Bleuel, E. J. Bond, D. K. Bradley *et al.*, Phys. Plasmas **19**, 056315 (2012).

[22] A. J. MacKinnon, N. B. Meezan, J. S. Ross, S. Le Pape, L. Berzak Hopkins, L. Divol, D. Ho, J. Milovich, A. Pak, J. Ralph *et al.*, Phys. Plasmas **21**, 056318 (2014).

[23] M. M. Marinak, G. D. Kerbel, N. A. Gentile, O. Jones, D. Munro, S. Pollaine, T. R. Dittrich, and S. W. Haan, Phys. Plasmas **8**, 2275 (2001).

[24] J. D. Moody, D. A. Callahan, D. E. Hinkel, P. A. Amendt, K. L. Baker, D. Bradley, P. M. Celliers, E. L. Dewald, L. Divol, T. Döppner *et al.*, Phys. Plasmas **21**, 056317 (2014).

[25] D. H. Froula, L. Divol, R. A. London, R. L. Berger, T. Döppner, N. B. Meezan, J. Ralph, J. S. Ross, L. J. Suter, and S. H. Glenzer, Phys. Plasmas **17**, 056302 (2010).

[26] J. D. Moody, P. Datte, K. Krauter, E. Bond, P. A. Michel, S. H. Glenzer, L. Divol, C. Niemann, L. Suter, N. Meezan *et al.*, Rev. Sci. Instrum. **81**, 10D921 (2010).

[27] M. Rosen *et al.*, High Energy Density Phys. **7**, 180 (2011).

[28] E. L. Dewald, K. M. Campbell, R. E. Turner, J. P. Holder, O. L. Landen, S. H. Glenzer, R. L. Kauffman, L. J. Suter, M. Landon, M. Rhodes *et al.*, Rev. Sci. Instrum. **75**, 3759 (2004).

[29] F. Ze, R. L. Kauffman, J. D. Kilkenny, J. Wielwald, P. M. Bell, R. Hanks, J. Stewart, D. Dean, J. Bower, and R. Wallace, Rev. Sci. Instrum. **63**, 5124 (1992).

[30] M. B. Schneider, O. S. Jones, N. B. Meezan, J. L. Milovich, R. P. Town, S. S. Alvarez, R. G. Beeler, D. K. Bradley, J. R. Celeste, S. N. Dixit *et al.*, Rev. Sci. Instrum. **81**, 10E538 (2010).

[31] S. P. Regan, N. B. Meezan, L. J. Suter, D. J. Strozzi, W. L. Kruer, D. Meeker, S. H. Glenzer, W. Seka, C. Stoeckl, V. Y. Glebov *et al.*, Phys. Plasmas **17**, 020703 (2010).

[32] H. F. Robey, P. M. Celliers, J. D. Moody, J. Sater, T. Parham, B. Kozioziemski, R. Dylla-Spears, J. S. Ross, S. LePape, J. E. Ralph *et al.*, Phys. Plasmas **21**, 022703 (2014).

[33] E. L. Dewald, C. Thomas, S. Hunter, L. Divol, N. Meezan, S. H. Glenzer, L. J. Suter, E. Bond, J. L. Kline, J. Celeste *et al.*, Rev. Sci. Instrum. **81**, 10D938 (2010).

[34] H. G. Rinderknecht, M. G. Johnson, A. B. Zylstra, N. Sinenian, M. J. Rosenberg, J. A. Frenje, C. J. Waugh, C. K. Li, F. H. Sguin, R. D. Petrasso *et al.*, Rev. Sci. Instrum. **83**, 10D902 (2012).

[35] J. Biener, D. Ho, C. Wild, E. Woerner, M. Biener, B. El-dasher, D. Hicks, J. Eggert, P. Celliers, G. Collins *et al.*, Nucl. Fusion **49**, 112001 (2009).

[36] J. Nuckolls, L. Wood, A. Thiessen, and G. Zimmerman, Nature (London) **239**, 139 (1972).

[37] D. T. Casey, V. A. Smalyuk, K. S. Raman, J. L. Peterson, L. Berzak Hopkins, D. A. Callahan, D. S. Clark, E. L. Dewald, T. R. Dittrich, S. W. Haan *et al.*, Phys. Rev. E **90**, 011102 (2014).

[38] D. S. Clark, J. L. Milovich, D. E. Hinkel, J. D. Salmonson, J. L. Peterson, L. F. Berzak Hopkins, D. C. Eder, S. W. Haan, O. S. Jones, M. M. Marinak *et al.*, Phys. Plasmas **21**, 112705 (2014).

[39] D. L. Bleuel, C. B. Yeamans, L. A. Bernstein, R. M. Bionta, J. A. Caggiano, D. T. Casey, G. W. Cooper, O. B. Drury, J. A. Frenje, C. A. Hagmann *et al.*, Rev. Sci. Instrum. **83**, 10D313 (2012).

[40] T. Ma, P. K. Patel, N. Izumi, P. T. Springer, M. H. Key, L. J. Atherton, L. R. Benedetti, D. K. Bradley, D. A. Callahan, P. M. Celliers *et al.*, Phys. Rev. Lett. **111**, 085004 (2013).

[41] C. Cerjan, P. T. Springer, and S. M. Sepke, Phys. Plasmas **20**, 056319 (2013).

[42] H. W. Herrmann, N. Hoffman, D. C. Wilson, W. Stoeffl, L. Dauffy, Y. H. Kim, A. McEvoy, C. S. Young, J. M. Mack, C. J. Horsfield *et al.*, Rev. Sci. Instrum. **81**, 10D333 (2010).